46. Degenerative Disk Disease I

Standard imaging techniques for the MR evaluation of the lumbar spine differ from those implemented in the cervical and thoracic regions. For axial imaging in the cervical region, GRE T2-weighted techniques are preferred, due to potential problems from CSF pulsation and the small size of cervical spinal structures warranting thin slice imaging (2-3 mm). In distinction, slice thicknesses of 3-4 mm are acceptable in imaging of the lumbar spine where less prominent pulsation artifact also favors the acquisition of FSE T2WI. A thick coronal saturation slab is also routinely placed over the prevertebral tissues to eliminate artifacts from the aorta and vena cava, as well as abdominal motion (if the phase encoding direction is anterior-posterior). FSE has other advantages over GRE, including—due to its additional 180 degree refocusing pulse—diminished artifacts arising from differences in tissue susceptibility. Such artifacts play a role clinically, not only in post-operative patients where metal implants may limit the diagnostic utility of GRE sequences, but also with respect to evaluation of spinal canal and neuroforaminal narrowing. With GRE sequences, susceptibility effects from bone may exaggerate canal or foraminal narrowing depending upon the selection of imaging parameters. Tissue contrast with FSE T1WI of the lumbar spine is derived from differences in SI between high SI epidural fat versus the low SI thecal sac contents and intervertebral disk. This contrast is lost somewhat on FSE T2WI due to the preservation of hyperintense fat signal on such sequences.

The MR appearance of the intervertebral disk changes with age. In the neonate and young child, the nucleus is very high signal intensity on T2WI and sharply demarcated from the annulus. The demarcation becomes less distinct with time, with the nucleus and inner annulus both high signal intensity but differentiated from the outer annulus with low signal intensity. In adolescents, a transverse fibrous plate appears along the equator of the disk, evident as a band of low SI, with this appearance persisting in adults.

With time, in the adult, and subsequent degenerative disease, various factors contribute to change the disk appearance further. The annulus for example may tear as illustrated in Figure 46.1. Here, sagittal (A) FSE T2WI demonstrates a disk bulge with a radial annular tear that has allowed high SI fluid and mucoid material (white arrow) to fill the resulting gap. (B) Axial T2WI illustrate mild resulting narrowing of the central spinal canal from the disk bulge, along with the aforementioned high SI (white arrow) material along the posterior disk margin. This hyperintense region typically enhances on CE T1WI. Tears (also called fissures) can be concentric, transverse or radial. Radial tears are those that extend from the nucleus into the annulus. Most annular tears are asymptomatic.

Although some loss of disk SI occurs normally with age, desiccation is the hallmark of

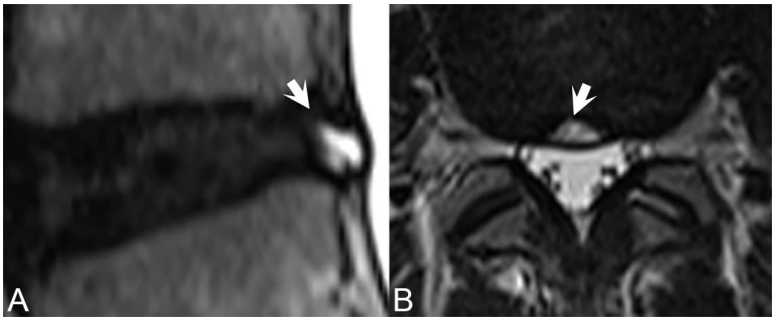

Fig. 46.1

degenerative disk disease. Disk desiccation occurs due to proteoglycan loss within the nucleus pulposus resulting in a diminished ability of that structure to attract water. Desiccated disks are more reliably detected on FSE imaging than on GRE due to the high fluid sensitivity of the latter. A relatively normal L2-3 disk is illustrated in Figure 46.2. On the (A) sagittal T1WI there is preservation of intervertebral disk height. On the (B) FSE T2WI a relatively normal hyperintense nucleus pulposus is noted, surrounded by the low SI annulus. Note, as well, the normal low signal intensity intranuclear cleft. In distinction, the L3-4 intervertebral disk demonstrates marked loss of height and SI, the latter evident by the uniformly low SI on (B) FSE T2WI. Severely degenerated disks may contain foci of gas, contents suggested in this case by the linear hypointensity within the disk on (A) T1WI. The lack of mobile protons within these likely nitrogen-containing gas pockets results in low SI on both T1 and T2WI. Figure 46.2 also illustrates mild end-plate degenerative changes at L3-4 (See Chapter 47) as well as a grade 3 anterolisthesis of L5 on S1. Grading of anterolistheses is based upon the degree of anterior displacement of the superior vertebral body. Grade 1 lesions consist of displacement less than 25% of vertebral body length, grade 2 lesions of displacement between 25 and 50%, and grade 3 lesions of displacement greater than 50%. The anterolisthesis in Figure 46.2 was associated with bilateral pars interarticularis defects—a finding better visualized on CT and present bilaterally in nearly all patients with grade 2 or 3 listheses. Pars defects are likely related to prior trauma, although a congenital etiology has also been suggested in the past. In the absence of pars defects, spondylolisthesis is typically accompanied by marked bilateral facet arthropathy. The L5-S1 intervertebral disk in Figure 46.2 rests superior to the posterior portion of S1 despite the anteriorly displaced L5 vertebrae. This portion of the disk does not extend significantly beyond the posterior border of S1 but appears to result in anteroposterior narrowing of the central spinal canal—a phenomenon known as a pseudo bulge. An anterolisthesis will also lead to elongated neural foramina in the AP dimension, narrowing them in the craniocaudal dimension. Although axial imaging is typically obtained with slices parallel to the intervertebral disk—in order to facilitate evaluation of

disk protrusions and associated canal stenoses—non-angled imaging planes (with acquisition of a continuous slice block) may aid in visualization of pars interarticularis defects.

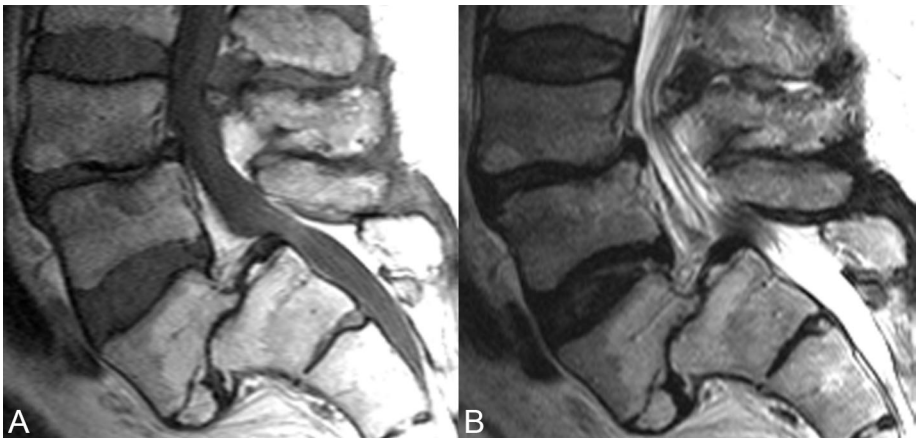

Fig. 46.2